A study of low-energy guest phonon modes in clathrate-II Na_xSi_{136} (x = 3, 23, and 24)

2010 J. Phys.: Condens. Matter 22 355401

(http://iopscience.iop.org/0953-8984/22/35/355401)

J. Phys.: Condens. Matter **22** (2010) 355401 (5pp) doi:10.1088/0953-8984/22/35/355401

A study of low-energy guest phonon modes in clathrate-II Na_xSi_{136} ($x = 3$, 23, and 24)

M Beekman[1], R P Hermann[2,3,4], A Möchel[2,3,4], F Juranyi[5] and G S Nolas[1,6]

[1] Department of Physics, University of South Florida, Tampa, FL 33620, USA
[2] Institute for Solid State Research, JCNS and JARA-FIT, Forschungszentrum Jülich GmbH, Jülich D-52425, Germany
[3] Department of Physics, University of Liège, B-4000 Liège, Belgium
[4] Department of Chemistry, University of Liège, B-4000 Liège, Belgium
[5] Laboratory for Neutron Scattering, ETH Zürich and Paul Scherrer Institut, CH-5232 Villigen-PSI, Switzerland

E-mail: gnolas@cas.usf.edu

Received 26 May 2010, in final form 13 July 2010
Published 10 August 2010
Online at stacks.iop.org/JPhysCM/22/355401

Abstract
Single-crystal x-ray diffraction from clathrate-II Na_xSi_{136} ($x = 24$) prepared by a new technique reveals the exceptionally large $Na@Si_{28}$ atomic displacement parameter (U_{eq}) is strongly temperature dependent, and can be attributed to low-energy rattling modes associated with the Na guest. Inelastic neutron scattering (INS) spectra collected from Na_xSi_{136} powder specimens ($x = 3$, 23) confirm the presence of low-energy guest-derived phonon modes for $Na@Si_{28}$ and $Na@Si_{20}$. The lower energy $Na@Si_{28}$ rattler mode falls in the frequency range of the silicon host acoustic phonons, indicating the possibility for interaction with these phonons. The presence of these low-energy modes combined with the ability to controllably vary the guest content presents a unique opportunity for exploring the influence of guest-framework interactions on the lattice dynamics in intermetallic clathrates.

1. Introduction

Intermetallic clathrate-I compounds have been identified [1, 2] as a promising class of candidate thermoelectric materials. The enhanced thermoelectric properties in these materials arise in large part from marked guest–host interactions. In particular, interactions between the host-framework acoustic phonons and those associated with the guest species give rise to intriguing lattice dynamics. Relatively weak guest–host bonding results in low-energy 'rattling' phonon modes associated with the encapsulated guests. These modes exhibit very little dispersion [3] and fulfill the criteria for localized modes, and can efficiently impede the lattice thermal conduction in these materials [4] through strong interaction with the heat carrying phonons.

In comparison to their clathrate-I counterparts, variants with the clathrate-II crystal structure have only recently begun to be explored more thoroughly. Although a rich phase space can be inferred, very few compositions are experimentally known [5]. Previously reported crystallographic [6], Raman scattering [7], and density functional theory [8] investigations have indicated rattling behavior in the stoichiometric (i.e. full guest occupation) $A_8Na_{16}E_{136}$ clathrates (A = Cs, Rb; E = Si, Ge). It is of interest to identify material systems exhibiting this behavior in which the guest content can be varied, allowing the influence of the guest dynamics to be systematically studied. Moreover, the thermal transport might be tuned by controlling composition in such systems. Here we report Na rattling behavior in the Na_xSi_{136} ($0 < x \leqslant 24$) system, as revealed from temperature-dependent single-crystal x-ray diffraction (XRD) and inelastic neutron scattering (INS). Considering the ability to fully vary the guest content in systems such as Na_xSi_{136} and the implications on thermal transport, these observations are of particular interest in the context of the search for novel thermoelectric clathrate materials.

2. Experimental details

Single crystals of $Na_{24}Si_{136}$ for temperature-dependent single-crystal XRD were prepared by a new method, in which phase-pure single crystals of the clathrate-II phase are grown

[6] Author to whom any correspondence should be addressed.

from a Na_4Si_4 precursor ingot by slow, controlled removal of Na, achieved via Na vapor phase intercalation of graphite. Both reactants (Na_4Si_4 and graphite) were sealed, spatially separated allowing only vapor exchange, in a stainless steel vessel under nitrogen and heated at 600 °C for 36 h. Further details of this new synthesis procedure will be reported elsewhere [9]. Temperature-dependent single-crystal x-ray diffraction intensity data from $Na_{24}Si_{136}$ were collected at 173, 220, and 295 K using Mo Kα radiation. The intensity data confirmed the clathrate-II crystal structure, which was refined within the $Fd\bar{3}m$ space group.

For INS experiments, two 9 g powder specimens of Na_xSi_{136} with $x = 3$ and 23, respectively, were prepared by thermal decomposition of Na_4Si_4 powder under dynamic vacuum (10^{-6} Torr), followed by heat treatment under dynamic vacuum at 420 °C for 24 h and 380 °C for 75 min for $x = 3$ and 23, respectively. Specimen composition was determined by Rietveld analysis, which established that in Na_3Si_{136} only the larger Si_{28} cages are (partially) occupied and the Si_{20} cages remain empty, while for $Na_{23}Si_{136}$ the Si_{28} cages are fully occupied and the Si_{20} cages are almost fully occupied. This is in agreement with the observation that for $x < 8$, Na almost exclusively occupies the Si_{28} cages; the Si_{20} cages show significant occupation only after all Si_{28} cages are completely filled [10]. The phase fractions of (clathrate-I) Na_8Si_{46} and (diamond structure) α-Si impurity phases commonly observed [10] in Na_xSi_{136} specimens were minimized in the specimens reported on here (approx. 2 wt% Na_8Si_{46} and 1 wt% α-Si for the Na_3Si_{136} specimen, and approx. 3 wt% Na_8Si_{46} for $Na_{23}Si_{136}$ specimen as determined by Rietveld refinement), so that any scattering contribution from these phases to the INS spectra would be minimized. The composition of both specimens was further analyzed using neutron prompt gamma activation at the PGAA spectrometer [11] (FRM II, Munich). The normalized Na content from this technique was estimated to be 4.9(5) and 22.9(5) for the Na_3Si_{136} and $Na_{23}Si_{136}$ samples, respectively, in qualitative agreement with the Rietveld analysis.

The inelastic scattering from Na_3Si_{136} and $Na_{23}Si_{136}$ powder at 298 K was measured on the cold neutron time-of-flight instrument FOCUS (SINQ, Villigen). The neutron wavelength was 4 Å and the phonon density of states (PDOS) was calculated in the incoherent scattering approximation from the scattering integrated over all detectors after subtraction of the empty container contribution. The data were normalized to sample mass and monitor counts. Prior to the measurements the samples were dried at 120 °C for 24 h in a vacuum oven; a small constant contribution was subtracted from the time-of-flight spectra in order to account for some residual scattering by hydrogen observed in the specimens.

3. Results and discussion

3.1. Temperature-dependent single-crystal x-ray diffraction from $Na_{24}Si_{136}$

There are three crystallographically distinct sites in the clathrate-II host-framework (8*a*, 32*e*, and 96*g*; space group $Fd\bar{3}m$), which form two distinct coordination polyhedra encaging the guests (at 8*b* and 16*c*). When allowed to refine, all Na and Si crystallographic sites showed full occupation (within 1σ) in accordance with the chemical composition $Na_{24}Si_{136}$ for the specimen. The room-temperature refined structural parameters for the $Na_{24}Si_{136}$ specimen in the present work agree very well (i.e. within 2σ) with those recently obtained from $Na_{24}Si_{136}$ single crystals prepared by spark plasma treatment [12].

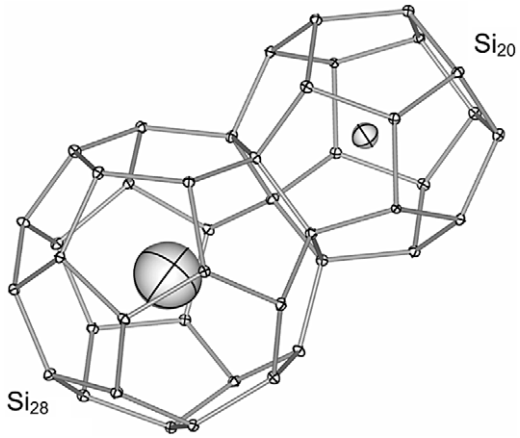

Figure 1. Crystal structure fragment showing the two caged Na guests in $Na_{24}Si_{136,}$ in the form of an ellipsoid plot of the atomic displacement parameters (drawn for 50% probability) determined from room-temperature single-crystal structure refinement.

The Na guest refined at the 8b crystallographic site in the Si_{28} cage exhibits an extremely large U_{eq}. This is illustrated by the ellipsoid representation shown in figure 1, calculated from room-temperature structure refinement, and can be understood in terms of the very large dissimilarity between the effective ionic radius [13] of Na and the free radius of the large Si_{28} cage. Moreover, U_{eq} for this site varies strongly with temperature, implying the disorder has a substantial dynamic component. The temperature dependent U_{eq} for Na@Si_{28} and Na@Si_{20}, extracted from the $Na_{24}Si_{136}$ single-crystal structure refinements, are plotted in figure 2, along with U_{eq} for Cs@Si_{28} and Rb@Si_{28} in $A_8Na_{16}Si_{136}$ (A = Cs, Rb) from [6].

Inasmuch as analytical expressions for the temperature dependence of U_{eq} can be obtained [12], the harmonic oscillator model provides a simple yet useful tool to gain insight from atomic displacement parameter analysis [14], especially for atomic vibrations that can be approximated by localized Einstein modes [15]. At temperatures such that the Einstein temperature $\Theta_E = h\nu/k_B < 2T$, where ν is the oscillator frequency, h is the Planck constant, and k_B is the Boltzmann constant, the simple classical relation $U_{eq}(T) = k_BT/[m(2\pi\nu)^2]$ can be expected to describe the temperature dependence of the atomic displacement parameter [16]. Fitting the data to this model as shown in figure 2, we obtain estimated oscillator energies $h\nu$ of 7.2 meV and 16.0 meV for Na@Si_{28} and Na@Si_{20}, respectively. The value for Na@Si_{28} is indicative of a low-energy phonon mode associated with this guest, and is comparable to rattler energies observed in clathrate-I compounds [17].

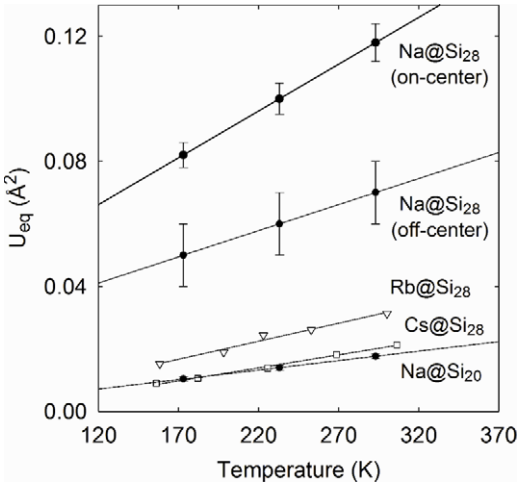

Figure 2. Temperature dependence of the Na atomic displacement parameters (U_{eq}), obtained from single-crystal XRD, along with those from Cs@Si$_{28}$ and Rb@Si$_{28}$ [6]. Error bars represent one estimated standard deviation (esd).

A substantial zero-temperature intercept of U_{eq} for Na at the 8*b* site suggests static disorder may also be present. An off-centered (positioned at the 32*e* site, i.e. four-fold split-site) model [18] could also be refined against the single-crystal data. As might be expected [19], U_{eq} from this model (figure 2) is somewhat reduced in magnitude, in both the zero-temperature intercept and temperature dependence (the oscillator energy $h\nu = 9.6$ meV for this model), yet both still remain relatively large. No significant improvement in the refinement residuals was obtained and difference Fourier maps revealed no unequivocal indication of off-centering for this guest in its pseudospherical cage. Model density functional theory investigations suggest either a flat, broad potential for Na in the Si$_{28}$ cage with the minimum in the cage center [20], or a very shallow minimum at approximately 0.5–1.0 Å away from the center [21]. In either case, at elevated temperatures thermal excitation will cause Na to dynamically explore the large volume of the Si$_{28}$ cage, in agreement with the strong temperature dependence of U_{eq} for the guest atom. Inelastic neutron scattering (INS) experiments on Na$_3$Si$_{136}$ and Na$_{23}$Si$_{136}$, which we now discuss, offer further insight into the physical nature of the Na disorder for Na@Si$_{28}$.

3.2. Inelastic neutron scattering from Na$_3$Si$_{136}$ and Na$_{23}$Si$_{136}$

The experimentally weighted PDOS of Na$_x$Si$_{136}$ with $x = 3$ and 23 determined from INS are shown figure 3. Comparison of the spectra reveals that increasing the Na content causes an overall softening and broadening of the Si framework modes [22] at 50–60 and 22 meV. This softening can be attributed to the increased mass per unit cell and the mixing of Na vibrational modes with those of the Si framework. We also note a slight increase in Si–Si bond lengths for Na$_{23}$Si$_{136}$ (refined cubic lattice parameter $a = 14.7173(2)$ Å) relative to Na$_3$Si$_{136}$ ($a = 14.6461(2)$ Å), induced by the occupation of the sixteen smaller Si$_{20}$ cages per conventional unit cell. Two prominent vibrational modes associated with

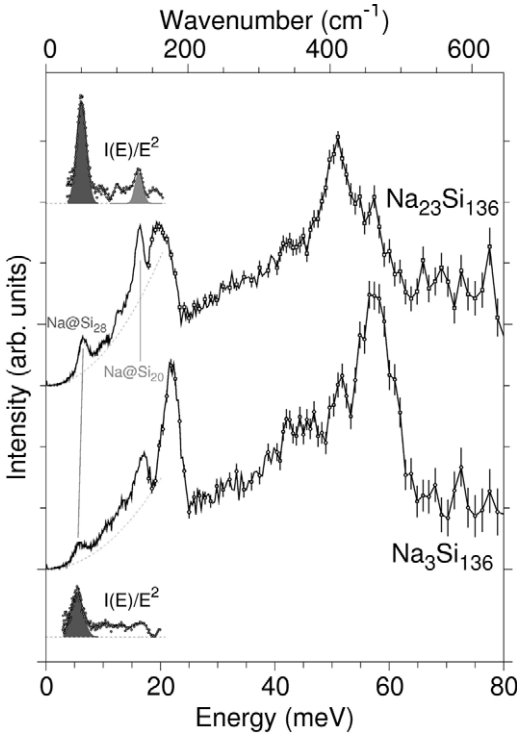

Figure 3. Experimental phonon density of states, $I(E)$, in Na$_{23}$Si$_{136}$ and Na$_3$Si$_{136}$ as deduced from INS. Insets: corresponding reduced PDOS, given as $I(E)/E^2$.

the Na guests are observed, in agreement with [23], and are labeled as Na@Si$_{20}$ and Na@Si$_{28}$ in figure 3. The data up to 20 meV was phenomenologically modeled by a sum of Gaussian contributions and a parabolic background (dashed lines in figure 3). The Na@Si$_{28}$ and Na@Si$_{20}$ derived modes are indicated by the dark gray and light gray shaded areas, respectively, in the reduced PDOS (insets). The features in the INS spectra and their assignments to the respective Na guests are consistent with the cage occupations obtained from Rietveld refinement. The fitting parameters from the model yield Na@Si$_{28}$ mode energies of 6.48(2) and 5.84(5) meV for $x = 3$ and 23, respectively, and 16.35(8) meV for the Na@Si$_{20}$ mode in $x = 23$. These Na phonon energies agree relatively well with those estimated above from the temperature-dependent Na U_{eq}. The full-widths at half-maximum of the Na@Si$_{28}$ modes are 2.4(1) meV and 1.96(3) meV for $x = 3$ and 23, respectively. The description of Na@Si$_{28}$ at the 8b site implies relatively high symmetry, such that the broadening of the mode associated with this guest can be interpreted as an indication of a shorter mean lifetime of these phonons. Although to our knowledge no theoretical reports of phonon spectra and/or lattice dynamics exist yet for Na$_x$Si$_{136}$, our conclusion appears to be supported by the single rattler frequency found from DFT calculations for other alkali guests in the pseudospherical Si$_{28}$ cage [8]. Shorter mean lifetimes may be indicative of an enhanced collision rate with acoustic phonons, and low lattice thermal conductivity can be expected in such cases. This relationship has been observed in other clathrate compounds [3, 4, 17] as well as the intermetallic Zn$_4$Sb$_3$ [24].

Table 1. Characteristic energies for guest-derived phonon modes in selected silicon clathrate-II compounds, as determined from temperature-dependent single-crystal XRD (U_{eq}), temperature-dependent heat capacity (C_p), inelastic neutron scattering (INS), Raman scattering, and density functional theory calculations (DFT).

Compound	Guest	Energy (meV)	Technique	Reference
$Na_{24}Si_{136}$	$Na@Si_{28}$	7.2	U_{eq}	This work
		4.8	C_p	[25]
	$Na@Si_{20}$	16.0	U_{eq}	This work
		14.3	C_p	[25]
$Na_{23}Si_{136}$	$Na@Si_{28}$	5.8	INS	This work
	$Na@Si_{20}$	16.4	INS	This work
Na_3Si_{136}	$Na@Si_{28}$	6.5	INS	This work
$Rb_8Na_{16}Si_{136}$	$Rb@Si_{28}$	6.8	U_{eq}	[6]
	$Na@Si_{20}$	16.1	U_{eq}	[6]
$Cs_8Na_{16}Si_{136}$	$Cs@Si_{28}$	6.6	U_{eq}	[6]
		7.1	Raman	[7]
		7.9	DFT	[7]
	$Na@Si_{20}$	17.4	U_{eq}	[6]
		14.6	DFT	[7]

3.3. Comparison with other silicon clathrate-II guests

The characteristic rattling energies estimated in the present work for the two distinct guests in Na_xSi_{136} ($x = 3$, 23, and 24) are compared in table 1 to rattling energies for guests in silicon clathrate-II phases estimated from various techniques [6, 7, 25]. The rattling energies for $Na@Si_{20}$ are comparable between compositions, indicating the local guest-framework interaction is similar in these different silicon clathrate-II compounds. In spite of the significantly smaller Na mass as compared to Rb and Cs, the estimated $Na@Si_{28}$ rattler energies are comparable to those for $Rb@Si_{28}$ and $Cs@Si_{28}$. We attribute this similarity in rattler energies to the significantly larger 'free space' available to the smaller ionic radius Na guest (i.e. resulting in a softer 'spring constant'), which is reflected in the much larger amplitude thermal motion for $Na@Si_{28}$ as compared to $Cs@Si_{28}$ or $Rb@Si_{28}$, revealed by the data of figure 2.

4. Conclusions

Inasmuch as the guest content can be controllably varied, clathrate-II phases offer ideal material systems for investigation of the interrelationships between the guest- and host-framework in intermetallic clathrates, and the implications of such relationships on the physical properties of these materials. To this end, high quality single-crystal and high purity polycrystalline specimens are of importance in order to investigate their intrinsic properties. Our temperature-dependent single-crystal XRD and powder INS investigations show unequivocally the presence of low-energy phonon modes associated with the Na guests. The $Na@Si_{28}$ mode is located within the frequency range of the host acoustic phonons [22], implying low lattice thermal conductivity values might be expected for these materials. The complement of these low-energy guest-atom phonon modes with the ability to fully vary the guest content in clathrate-II phases, in contrast to other intermetallic clathrates, may offer a path to tune the thermal properties of intermetallic clathrate materials. These aspects, coupled with the complex clathrate-II crystal structure resulting in inherently low lattice thermal conductivities [26, 27] and the possibility to influence electronic structure via framework substitution [28, 29], motivate a more intense exploration of the thermoelectric properties of intermetallic clathrate-II compounds. Detailed theoretical calculations of the lattice dynamics in the Na_xSi_{136} and related clathrates will be of particular interest.

Acknowledgments

MB and GSN acknowledge support from US DOE Grant No. DE-FG02-04ER46145 for crystal growth and specimen preparation, as well as characterization and data analysis. MB acknowledges support from the University of South Florida Presidential Doctoral Fellowship. This work is based on experiments performed at the Swiss spallation neutron source SINQ, Paul Scherrer Institute, Villigen, Switzerland. The FRM-2 is acknowledged for provision of the neutron beamtime on PGAA, and Ms Lea Canella is acknowledged for assistance during the data acquisition. The authors kindly thank Kenneth I. Hardcastle of Emory University and Angus P Wilkinson of Georgia Institute of Technology for single-crystal x-ray diffraction data collection. Single-crystal structure refinements were carried out with the aid of the SHELX [30] and WinGX [31] software. Rietveld refinements were carried out with the aid of the GSAS [32] and EXPGUI software [33]. Figure 1 was drawn using the VESTA software [34].

References

[1] Slack G A 1997 *Mater. Res. Soc. Symp. Proc.* **478** 47
[2] Nolas G S, Cohn J L, Slack G A and Schujman S B 1998 *Appl. Phys. Lett.* **73** 178
[3] Dong J J, Sankey O F and Myles C W 2001 *Phys. Rev. Lett.* **86** 2361
[4] Cohn J L, Nolas G S, Fessatidis V, Metcalf T H and Slack G S 1999 *Phys. Rev. Lett.* **82** 779
[5] Beekman M and Nolas G S 2008 *J. Mater. Chem.* **18** 842
[6] Nolas G S, Vanderveer D G, Wilkinson A P and Cohn J L 2002 *J. Appl. Phys.* **91** 8970
[7] Nolas G S, Kendziora C A, Gryko J, Dong J J, Myles C W, Poddar A and Sankey O F 2002 *J. Appl. Phys.* **92** 7225
[8] Myles C W, Dong J J and Sankey O F 2003 *Phys. Status Solidi* b **239** 26
[9] Stefanoski S, Beekman M and Nolas G S, in preparation
[10] Beekman M, Nenghabi E N, Biswas K, Myles C W, Baitinger M, Grin Yu and Nolas G S 2010 *Inorg. Chem.* **49** 5338
[11] Kudejova P *et al* 2009 The new PGAA installation at the FRM II *Capture Gamma-Ray Spectroscopy and Related Topics: Proc. 13th Int. Symp. Capture Gamma-Ray Spectroscopy and Related Topics* vol 1090, pp 89–96 http://link.aip.org/link/?APC/1090/89/1
[12] Beekman M, Baitinger M, Borrmann H, Schnelle W, Meier K, Nolas G S and Grin Yu 2009 *J. Am. Chem. Soc.* **131** 9642
[13] Shannon R D 1976 *Acta Crystallogr.* A **32** 751
[14] Willis B T M and Pryor A W 1975 *Thermal Vibrations in Crystallography* (Cambridge: Cambridge University Press)
[15] Dunitz J D, Schomaker V and Trueblood K N 1988 *J. Phys. Chem.* **92** 856

[16] Sales B C, Chakoumakos B C, Mandrus D and Sharp J W 1999 *J. Solid State Chem.* **146** 528
[17] Hermann R P, Schweika W, Leupold O, Rüffer R, Nolas G S, Grandjean F and Long G J 2005 *Phys. Rev.* B **72** 174301
[18] Brunet F, Mélinon P, San-Miguel A, Kéghélian P, Perez A, Flank A M, Reny E, Cros C and Pouchard M 2000 *Phys. Rev.* B **61** 16550
[19] Nolas G S, Weakley T J R, Cohn J L and Sharma R 2000 *Phys. Rev.* B **61** 3845
[20] Conesa J C, Tablero C and Wahnon P 2004 *J. Chem. Phys.* **120** 6142
[21] Libotte H, Gaspard J-P, San Miguel A and Mélinon P 2003 *Europhys. Lett.* **64** 757
[22] Tang X, Dong J J, Hutchins P, Shebanova O, Gryko J, Barnes P, Cockcroft J K, Vickers M and McMillan P F 2006 *Phys. Rev.* B **74** 014109
[23] Mélinon P *et al* 1999 *Phys. Rev.* B **59** 10099
[24] Schweika W *et al* 2007 *Phys. Rev. Lett.* **99** 125501
[25] Beekman M, Schnelle W, Bormann H, Baitinger M, Grin Yu and Nolas G S 2010 *Phys. Rev. Lett.* **104** 018301
[26] Beekman M and Nolas G S 2006 *Physica* B **383** 111
[27] Nolas G S, Beekman M, Gryko J, Lamberton G A Jr, Tritt T M and McMillan P F 2003 *Appl. Phys. Lett.* **82** 910
[28] Beekman M, Wong-Ng W, Kaduk J A, Shapiro A and Nolas G S 2007 *J. Solid State Chem.* **180** 1076
[29] Biswas K and Myles C W 2007 *Phys. Rev.* B **75** 245205
[30] Sheldrick G M 2008 *Acta Crystallogr.* A **64** 112
[31] Farrugia L J 1999 *J. Appl. Crystallogr.* **32** 837
[32] Larson A C and Von Dreele R B 2004 General structure analysis system (GSAS) *Los Alamos National Laboratory Report LAUR* 86–748
[33] Toby B H 2001 *J. Appl. Crystallogr.* **34** 210
[34] Momma K and Izumi F 2008 *J. Appl. Crystallogr.* **41** 653